Journal of Sensor Science and Technology
Vol. 28, No. 6 (2019) pp. 341-344
http://dx.doi.org/10.5369/JSST.2019.28.6.341
pISSN 1225-5475/eISSN 2093-7563

Impact of Electric Field on Propagation Velocity of Phase Boundary Between Nematic and Isotropic Phases of 5CB Liquid Crystal

Mohammad Awwal Adeshina[1], Mareddi Bharath Kumar[1], Daekyung Kang[1], Bongjun Choi[2], and Jonghoo Park[1,+]

Abstract

Liquid crystal (LC) mesophase materials manifest a variety of phase transitions. The optical properties of LCs are highly dependent upon the phase and orientation of the optical axis with respect to the polarization of incoming light. Studying the LC phase transitions is significantly important for a wide range of scientific and industrial applications. In this study, we demonstrate the propagation velocity of the phase boundary between the nematic and isotropic phase of 4-Cyano-4-pentylbiphenyl (5CB) liquid crystal for different electric fields using a polarized optical microscope. The results demonstrate that the propagation velocity of the phase boundary exhibits a peak value for a specific voltage, attributed to the supercooling of the isotropic phase of the LC. The analysis of the propagation velocity for different electric fields also provides a simple optical platform to measure the thermal anisotropy and voltage dependent thermal properties of the homogeneously aligned LC.

Keywords: Liquid Crystals, Phase transitions, 5CB, Temperature sensors

1. INTRODUCTION

Liquid crystals (LCs) are a stable phase of matter characterized by anisotropic properties without the existence of a three-dimensional crystal lattice, generally lying between the solid and isotropic "liquid" phase[1,2]. It differs from liquid because its molecules possess anisotropic orientational order, which means the properties of the LC is dependent on the direction which they are measured. Owing to its unique anisotropic optical and electro-optic properties, the LC mesophase materials have attracted attention not only from optical applications. including optical switches [3,4], electro-optic filters [5], digital data storage devices [6], holography[7-9], lenses [10,11], and computer displays [12], but also from sensor applications, including temperature sensors [13] and gas sensors [14,15]. The nematic to isotropic phase transition of LC is of importance for design of LC-based electro-optic devices. Various studies on the phase transition behavior of LC have been performed; however, much has not been done to investigate the impact of the electric field on the phase transition of LC. Here, we investigate the propagation velocity of the phase boundary between the nematic and isotropic phases, as a function of the voltage applied to the LC using a polarized optical microscope (POM). We found that the propagation velocity of the phase boundary between the nematic and isotropic phases, which can be translated to thermal diffusivity, can be modulated by the electric field applied to the LC and exhibits a peak value for a specific electric field, attributed to the supercooling of the isotropic phase of the LC. Measuring the propagation velocity of the phase boundary for different electric fields offers a simple optical method to measure the electro-thermal properties and thermal anisotropy of the homogeneously aligned LC.

[1]Department of Electrical Engineering, Kyungpook National Unversity.
E8-304, Kyungpook National University, 80 Daehak-ro, Buk-gu, Daegu, Korea
[2]Electro-optical Systems Team 2, Hanwha systems
188 Pangyo station, Bundang-gu, Seongnam, Gyeonggi-do, Korea
[+]Corresponding author: jonghoopark@knu.ac.kr
(Received: Sep. 25, 2019, Accepted: Oct. 21, 2019)

2. EXPERIMENTAL

2.1 Materials

The liquid crystal 4-Cyano-4-pentylbiphenyl (5CB) (CH_3-$(CH_2)_4$-C_6H_4-C_6H_4-CN) was purchased from Instec Inc. with a stated purity level greater than 99.5%. The indium tin oxide (ITO) coated polyethylene terephthalate (PET) and polyvinyl alcohol (PVA) were purchased from Sigma-Aldrich.

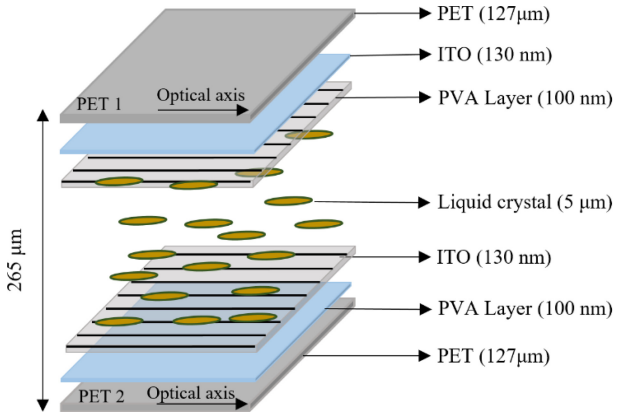

Fig. 1. Structure of LC sandwiched between two ITO coated PET substrates. The LC is homogeneously aligned along the optical axis of the PET substrates.

2.2 DESIGN AND FABRICATION

Figure 1 illustrates the structure of the LC cell sandwiched between two ITO coated PET substrates. The thicknesses of the PET film and ITO were 127 μm and 130 nm, respectively. The ITO coated PET films were first cleaned using ultrasonication for 5 min in acetone, IPA, and deionized water. The substrates were exposed to UV ozone for 20 min. The solution with 2 wt% PVA in DI water was deposited on the substrates and spin coated for 30s at a speed of 3000 rpm. The PVA coated substrates were baked for 1h at 90 °C on a hot plate. The PVA layers were rubbed in an antiparallel direction along the optical axis of the PET films. A 5 μm-thick double-sided adhesive tape was used to assemble the two PET substrates. The 5CB was filled between the substrates through the capillary action, in the isotropic phase.

3. RESULTS AND DISCUSSIONS

The LC cell was placed on the polarized optical microscope. The direction of the optical axis of the LC cell was 45° with respect to the optical axes of the polarizer and analyzer in the POM. A heater is attached to one end of the LC cell, which increases the temperature up to 55 °C in 10s. The velocity of the moving phase boundary between the nematic and isotropic phases, which can be translated into the thermal diffusivity of the LC, was measured when different voltages were applied to the LC cell. The bipolar pulse with a frequency of 100 Hz and zero DC bias was applied to the LC and exhibited a peak-to-peak voltage range of 0-8 V with an increment of 0.5 V. The changes in the structural texture of the LC and phase transition velocities for different voltages and heat were monitored using a POM and recorded by a CCD camera.

Figure. 3a depicts the POM image of the homogeneously aligned LC at the nematic phase under thermal equilibrium with the polarizer and analyzer set at 90°C to each other. Figure. 3b illustrates the crossed POM image of the phase boundary between the nematic and isotropic phases of the LC. The phase transition temperature of 5CB is 35.2 °C. The phase transition boundary is clearly observed and the moving direction of the phase boundary is from the side where the heater was placed to the opposite side. When the direction of the optical axis of the LC is aligned to 45°with respect to the optical axes of the crossed polarizers and the LC is at the isotropic phase, the light transmission through the crossed polarizer is zero, resulting in a dark color on the CCD. However, in our experiment, the isotropic phase still shows light transmission through the crossed polarizer. This effect is mainly due to the birefringence property of the PET substrates.

Figure 4 depicts the propagation velocity of the phase boundary when the direction of heat flow is in parallel (red circle) and perpendicular (black square) to the optical axis of the LC for different voltages. The thermal conductivity of the LC for a voltage of 1.5 V_{pp} exhibited a peak value. We attribute the propagation velocity peak for the voltage of 1.5 Vpp to the supercooling of the isotropic phase of the LC [16]. Additionally, the thermal conductivity of the LC along the optical axis was higher than that perpendicular to the optical axis, indicating

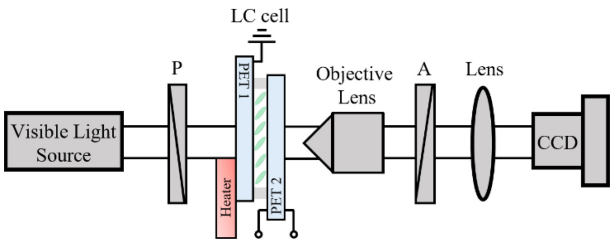

Fig. 2. Thermal diffusivity measurement setup, with the LC cell placed on the stage of the polarized optical microscope.

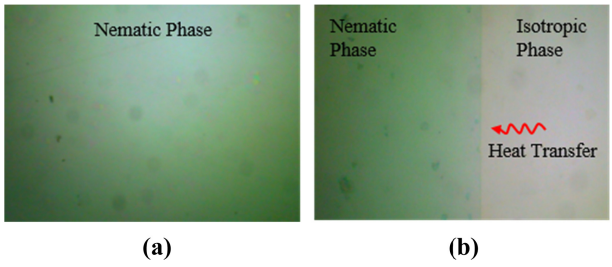

Fig. 3. POM images of 5CB during the nematic-isotropic phase transition (a) Nematic 5CB LC under thermal equilibrium, (b) 5CB LC under phase transition.

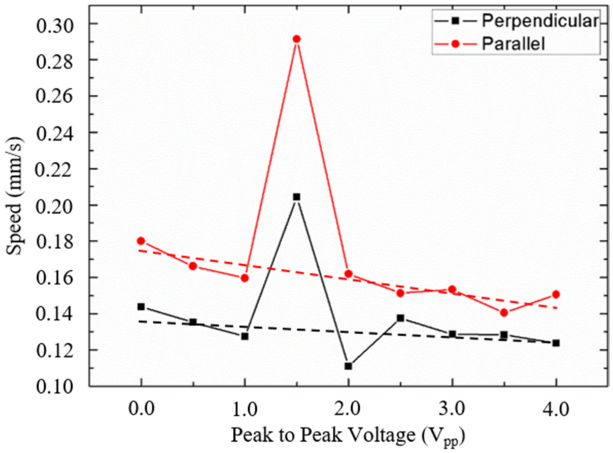

Fig. 4. Propagation velocity of the phase boundary between the nematic and isotropic phases as a function of voltage.

thermal anisotropy. The speed of the phase boundary propagation along the optical axis of the LC decreased as the voltage applied to the LC increased except at 1.5 V. When subjected to an alternating electric field, the LC was polarized and gained dipole moments, resulting in the rotation of the optical axis of the LC. The torque applied to the LC aligned the optical axis of the LC along the electric field. When a high electric field is applied to the LC whose optical axis is aligned parallel to the direction of the heat flow under zero electric field, the optical axis of the LC becomes perpendicular to the direction of heat flow. This makes the heat feel the perpendicular thermal conductivity, resulting in a decrease in the propagation velocity as the electric field increases. When the high electric field is applied to the LC whose optical axis is aligned perpendicular to the direction of heat flow under zero electric field, the optical axis of the LC remains perpendicular to the direction of the heat flow, resulting in an electric field independent of thermal conductivity. However, there is a slight decrease in the propagation velocity as the electric field increases. We attribute this slight decrease to the increased nematic to isotropic phase transition temperature. The phase transition temperature is proportional to the order parameter, which in turn increases as the voltage increases. The dashed lines represent the linear fit of the propagation velocity calculated without the data point for 1.5 V_{pp}. The slopes of the linear fit for the parallel and perpendicular alignment are –0.007 and –0.003, respectively. For the parallel alignment, both the increased order parameter and thermal anisotropy play a role in decreasing the propagation velocity, whereas for the perpendicular alignment, the increased order parameter affects the propagation velocity for different electric fields. Therefore, the slope of the parallel alignment is steeper than that of the perpendicular alignment.

4. CONCLUSIONS

In this study, we demonstrated the propagation velocity of the phase boundary between the nematic and isotropic phases of 5CB LC for different electric fields. We found that the propagation velocity of the phase boundary exhibits a peak for a specific electric field, attributed to the supercooling of the isotropic phase of the LC. Our simple experimental setup is used to measure not only the supercooling state of the isotropic phase but also the thermal anisotropy of the LC. Furthermore, we demonstrated the electric field dependent thermal properties of the LC using an optical method.

ACKNOWLEDGMENT

This work was supported by Hanwha systems.

REFERENCES

[1] S. Singh and D. A. Dunmur, *Liquid crystals: fundamentals*, World Scientific, City, 2002.
[2] S. Singh, “Phase transitions in liquid crystals”, *Phys. Rep.,* Vol. 324, No. 2-4, pp. 107-269, 2000.
[3] B.-X. Li, V. Borshch, S. V. Shiyanovskii, S.-B. Liu, and O. D. Lavrentovich, “Electro-optic switching of dielectrically negative nematic through nanosecond electric modification of order parameter”, *Appl. Phys. Lett.,* Vol. 104, No. 20, pp. 201105, 2014.
[4] B.-X. Li, V. Borshch, S. V. Shiyanovskii, S.-B. Liu, and O. D. Lavrentovich, “Kerr effect at high electric field in the isotropic phase of mesogenic materials”, *Phys. Rev. E,* Vol. 92, No. 5, pp. 050501, 2015.
[5] S.-T. Wu, “Design of a liquid crystal based tunable electrooptic filter”, *Appl.Opt.,* Vol. 28,No. 1, pp. 48-52, 1989.
[6] M. Eich and J. Wendorff, "Device for reversible optical data storage using polymeric liquid crystals", U. S. Patent 5,024,784, 18 Jun., 1991.
[7] Y. Zhao, L. Cao, H. Zhang, W. Tan, S. Wu, Z. Wang, Q. Yang, and G. Jin, “Time-division multiplexing holographic display using angular-spectrum layer-oriented method”, *Chinese Opt. Lett.,* Vol. 14, No. 1, pp. 010005-10009, 2016.
[8] M. Eich and J. H. Wendorff, “Erasable holograms in polymeric liquid crystals,” *Die Makromol. Chem., Rapid Commun.,* Vol. 8, No. 9, pp. 467-471, 1987.
[9] A. G. Chen and D. J. Brady, “Real-time holography in azo-dye-doped liquid crystals”, *Opt. Lett.,* Vol. 17, No. 6, pp. 441-443, 1992.
[10] P. Bos, D. Bryant, L. Shi, and B. Wall, "Tunable electro-optic liquid crystal lenses having resistive bridges and methods for forming the lenses”, U. S. Patent 9,280,020, 8 Mar., 2016.

[11] Y.-J. Wang, X. Shen, Y.-H. Lin, and B. Javidi, "Extended depth-of-field 3D endoscopy with synthetic aperture integral imaging using an electrically tunable focal-length liquid-crystal lens", *Opt. Lett.,* Vol. 40, No. 15, pp. 3564-3567, 2015.
[12] S. Ackley and P. Maltseff, "Dual screen display for mobile computing device", U. S. Patent 2016/0140931, 19 Mar., 2016.
[13] V. Balasubramaniam and S. Sastry, "Use of liquid crystals as temperature sensors in food processing research", *J. food Eng.,* Vol. 26, No. 2, pp. 219-230, 1995.
[14] Y. Han, K. Pacheco, C. W. Bastiaansen, D. J. Broer, and R. P. Sijbesma, "Optical monitoring of gases with cholesteric liquid crystals", *J. Am. Chem. Soc.,* Vol. 132, No. 9, pp. 2961-2967, 2010.
[15] Y.-T. Lai, J.-C. Kuo, and Y.-J. Yang, "A novel gas sensor using polymer-dispersed liquid crystal doped with carbon nanotubes", *Sens. Actuators A Phys.,* Vol. 215, pp. 83-88, 2014.
[16] G. Basappa and N. Madhusudana, "Effect of strong electric fields on phase transitions in some liquid crystals", *Mol. Cryst. Liq. Cryst. Sci. Technol. Sect. A. Mol. Cryst. Liq. Cryst.,* Vol. 288, No. 1, pp. 161-174, 1996.